

# NanoWalker: a fully autonomous highly integrated miniature robot for nano-scale measurements

Sylvain Martel, Peter Madden, Luke Sosnowski, Ian Hunter, and Serge Lafontaine

Bio-Instrumentation Laboratory, Department of Mechanical Engineering, Massachusetts Institute of Technology, 77 Massachusetts Ave., RM 3-147, Cambridge, MA, 02139, USA

## ABSTRACT

The aim of this project is to develop the smallest and most sophisticated wireless fully autonomous instrumented robot capable of subatomic movements. The robot named "NanoWalker" should bring a new paradigm in the way instruments are built while providing a sophisticated platform for a new range of applications. The project involves primarily the investigation of a new legged locomotion based on piezo-actuators with advanced micro-assembly techniques applied to complex embedded electronic systems; the development of new miniature instruments, micro-manipulators, integrated behavior for controlling, searching and scanning at the atomic scale; and the development of a subatomic navigation system. Besides all the new technologies and techniques that we intend to develop and which will be applicable to many areas and systems, the NanoWalker should provide a suitable yet more flexible and powerful platform compared to traditional macro-scaled instruments. It is anticipated that this new form of highly integrated autonomous microsystem will be used as the main building block for a new generation of measurement and inspection systems. In this paper, the main components of the NanoWalker are briefly described.

**Keywords:** NanoWalker, nano-scale, miniature robot, instrument, piezo-actuator, scanning tunneling microscope, flip-chip, flexible printed circuit

## 1. INTRODUCTION

Tele-robotics systems have several advantages. They allow humans to operate robots in hazardous and hostile environments and allow experts to manipulate objects and gather information at a distance. One of the objectives of this project is tele-nanorobotics where tele-robotics is pushed much further to allow humans to directly sense and manipulate the nano-scale world. Although the nano-scale imaging technologies such as the scanning tunneling microscope (STM) and atomic force microscope (AFM) are relatively well established, nano-scale manipulation and fabrication technologies are still at an early stage of research. At the present time, all competitive systems under investigation are macro-scale systems capable of nano-scale operations. The macro-scale approach imposes some severe limitations on the number of operations that can be performed on a small surface area due mainly to congestion between mechanical parts attached to an instrument frame within a very restricted working space. To resolve such issues, we propose a more homogeneous and modular approach by implementing small autonomous robots, each carrying an inter-changeable nano-scale imaging device, instrument, or nano-manipulator. Expansion in a system's performance and capability can be easily achieved by adding more NanoWalkers with similar or different inter-changeable devices. The ease of adapting such a system for nano-scale measurement and manipulations cannot be achieved with conventional approaches.

The impact should be a faster and more versatile technology for synthesizing and testing very large numbers of chemical and biological compounds and material including polymers, smart materials, and drugs. NanoWalker functions may include chemical dispensing and sampling, temperature measurement, and chemical, mechanical, optical and electrical impedance spectroscopy. Other potential applications include cell or gene manipulation and huge possibilities in the 3-D fabrication of nano-devices.

## 2. OVERVIEW

The NanoWalker is a very small wireless autonomous robot capable of carrying a variety of instruments. The first instrument that we are developing is an inter-changeable scanning tunneling microscope (STM). The instrumented robot will be capable of surface scanning with a resolution on the order of nanometers and fast displacement between two distant samples. The NanoWalker is based on piezo actuation and advanced electronics. A general block diagram of the NanoWalker is shown in Fig. 1. A 4 million bits per second (Mb/s) infrared (IR) communication interface, a 50 million instructions per second (MIPS) embedded digital signal processor (DSP) with 128 Kbytes (KB) of flash random access memory (RAM) and fast static RAM (SRAM) provide the support for the communication, processing, control, and systems management. Several 16-bit digital-to-

analog (D/A) converters (DAC) and power amplifiers drive the piezo tubes. An ultra low input bias current amplifier, a 16-channel analog multiplexer and a 16-bit analog-to-digital (A/D) converter are used for data acquisition. A proprietary controller and various advanced electronic devices perform the remaining tasks. All electronic devices are mounted with the most advanced packaging technology available to achieve the highest level of miniaturization.

## General Block Diagram

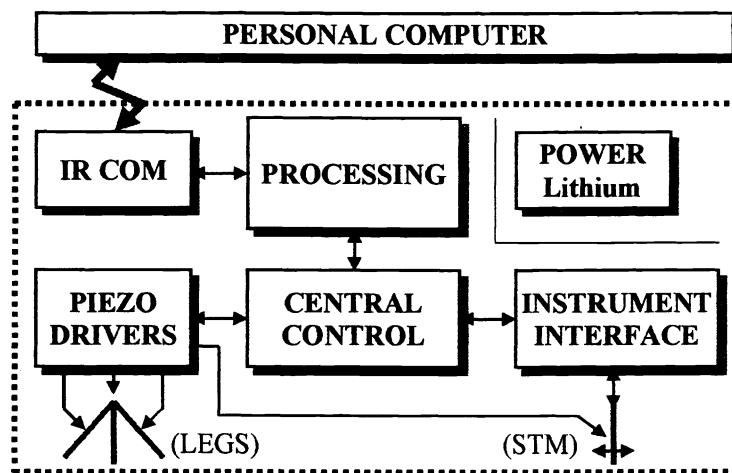


Fig. 1 - General block diagram of the NanoWalker.

By outfitting several NanoWalkers each with its own type of instrument, multiple measurements can be made simultaneously on multiple samples. Such homogeneity allows us to easily expand and/or tailor measurements without the restrictions imposed by the conventional approach in which a sample is mounted on an instrument chassis.

The NanoWalker has been designed to provide a standard platform for various types of instruments. Presently, the main mechanical frame is based on three piezo tubes forming an apex pointing upward and terminated with ruby balls making contact with the surface. This tripod allows fast displacement of the NanoWalker and acts as the mechanical support for the electronics. On the wireless version of the NanoWalker, a Kapton flexible printed circuit (FPC) interconnecting the electronic components is mounted vertically on the mechanical chassis. The components in die form are mounted on a pre-bumped FPC using flip-chip technology. The bumping process is not performed on the wafer, as typically done for high-volume production but rather on the FPC itself. The flip-chip approach allows significant space-saving compared to wire bonding. Careful placement is critical to avoid thermal problems. For instance, no high-powered components can be soldered on the bottom layer of the FPC (which faces the piezo tubes) to avoid temperature variation surrounding the sensitive precision instrument mounted between the piezo tubes.

The inter-changeable scanning tip of the STM is mounted on an additional piezo tube located at the center of the tripod. The inter-changeable instrument is fixed to the NanoWalker by a special micro-clamping configuration. A special 0.2 mm thick standard FPC-based miniature cable is used to provide the electrical link between the instrument and the NanoWalker. One end of the miniature cable is permanently connected to the instrument, the other end is inserted in a 0.3 mm pitch FPC connector located at the bottom layer of the NanoWalker FPC. A slide/hinge style actuator enables easy FPC insertion and extraction.

The NanoWalker development process is based on hardware/software co-design and verification methodology partitioned into three phases. This approach provides us with highly predictable results. During phase one, each is tested and characterized independently using more conventional computer interface boards. Based on the satisfactory results obtained during phase one, a first fully integrated but larger system implemented on a rigid printed circuit board (PCB) for hardware/software verification and validation is developed during phase two. Upon satisfactory results obtained in the second phase, an exact copy of the electronic circuit is implemented at the final miniaturization scale.

The final result will be a new form of highly integrated autonomous microsystem that can be used as the main building block for a new generation of measurement and inspection systems. By using the NanoWalker technology, an instrumentation system should become highly scalable and flexible.

### **3. INITIAL TECHNICAL ISSUES AND SCOPE OF THE PROJECT**

The first challenge for this project is to make a wireless version of the present tethered NanoWalker while minimizing its physical size. It was found through prior experimentation that the wires connecting to the robot impose some severe limitations and constraints on the accuracy of its motion. A wireless version requires the implementation of a complete computer system with all its memory, communication interface, and all the electronics required to control the piezo-actuators as well as providing a suitable interface for various instruments and nano-manipulators. Minimizing its physical size would mean that more NanoWalkers could work simultaneously within the same space. Besides a fair amount of electronics that must be embedded onto the NanoWalker to perform several sophisticated tasks simultaneously at a high rate, additional computation capability must be embedded because of limited bandwidth and long latency in wireless communication. This issue calls for the best micro-assembly techniques available and accessible for low volume production. Another technical issue related to the miniature size of the electronics is that testing with conventional techniques will not be possible. Thus built-in self test (BIST) procedures should be embedded within the robot. Implementing such a large amount of analog and digital electronics in such a small space while minimizing coupling noise and temperature fluctuation is another challenge. Furthermore, the flash memory and the programmable device containing custom hardware functions must be programmed while resident in the system. Hence, new in-system programming (ISP) accessories and techniques applicable to miniaturized systems must be developed.

Another major challenge of this project is the power source. Several alternatives have been evaluated so far from wireless power transmission to new lithium-based battery design. Because of the movement of the robot, efficiency in wireless power transmission (35 GHz microwaves for instance) is hard to maintain at an acceptable level. With the battery option, maintaining a small physical size while providing both sufficient operational time and drain current is the main challenge.

Another difficult aspect of this project is the large dynamic range of the positioning and navigation system mainly because the NanoWalker is capable of displacement over a long distance (up to 1.0 meter within the IR communication area) while nano-scale positioning accuracy is essential for many applications.

In summary, in order to provide an acceptable platform for various tasks, the NanoWalker must have an on-board computing system with specialized electronic interfaces. The whole physical implementation must be as small as possible to maximize the number of NanoWalkers that can work simultaneously within a given workspace. The robot must be wireless in order to improve its motion and avoid congestion when several robots move within a constrained space. Due to the amount of information that must be transmitted and received, the wireless technology used must be bi-directional and capable of high transmission rate. The robot must be capable of moving relatively fast using small steps. This is critical in order to achieve the dynamic range and accuracy in motion required for nano-scale positioning. Finally, a special standard interface must be developed to accept a variety of inter-changeable nano-instruments and nano-manipulators.

### **4. LOCOMOTION**

Based on the primary tests, the whole software for controlling the piezo-actuators has been re-written and revised. New functionality has been embedded to allow more control on the shape of the signals applied to the actuators as well as the synchronization between each actuator. A new graphical user interface (GUI) linked to this control software and a high-performance computer-based interface electronic board have been developed to allow further experiments to be conducted.

Indeed, we have conducted a large number of experiments to analyze the NanoWalker behavior and to determine the parameters and waveforms to achieve the best locomotion such as walking and rotating. Although much work needs to be done, we have already achieved under open-loop control conditions very good results in both walking and rotating in any given directions and speed. Indeed, displacement of at least 200 times ( $> 200$  mm/s) the initial speed has been achieved with more than 4000 steps (each step requires a special waveform made of several voltage outputs generated by the processor) performed per second with each step having a displacement of 5 micrometers ( $\mu\text{m}$ ).

## 5. MECHANICAL STRUCTURE

A diagram of the mechanical structure<sup>1</sup> of the first version of the NanoWalker is shown in Fig. 2. The basic mechanical structure is based on three piezo-ceramic tubes arranged in a conical shape with the apex pointing upward. Compared with other actuator technologies, piezo-ceramic actuation is very attractive for small robots because they have no moving parts to wear or degrade, have very high response speed, and consume virtually no power. Each tube acting as the robot leg is terminated at the base with a ruby ball. Each tube has four axial segmenting electrodes arranged as four 90 degree quadrants along the tube. The piezo-ceramic tube actuators operate by changing dimensions in response to an applied electric field. The voltage applied to the electrodes determines the magnitude of motion. Several combinations of voltage amplitudes applied to all electrodes among the three legs produce length motion, diameter length motion, and/or rapid multi-axis bending motions resulting in walking, rotating, and/or raster scanning. The general waveform applied to the piezo-tubes has a sharp transition followed by a smoother transition. The sharp transition allows the legs to slip on the surface and the smooth transition allows the legs to stick to the surface. Ideally, the combination of the sharp and smooth transitions will determine how many steps will be performed per second. Minimizing the total length of the waveform will increase the displacement speed. Unfortunately, if the first transition is too accentuated, the legs literally bounce and accuracy in motion is lost. Similarly, the second transition must be smooth enough to avoid slippage, which would also impact the accuracy in motion

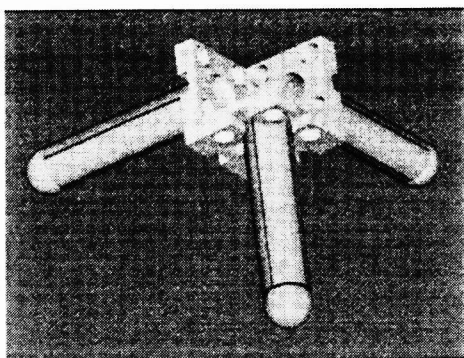


Fig. 2 - Basic mechanical structure.

A new mechanical structure has been developed. The new structure has better tolerances than the preceding one and the facility to accept the first instrument: a NanoWalker STM tip. The new platform also uses three piezo-actuator legs, each with an approximated length of 20 m and has been wired and tested successfully.

## 6. WIRELESS COMMUNICATION

Experimentation with NanoWalker motion has shown, without any doubt, that the tethered version cannot achieve the accuracy and repeatability of the NanoWalker displacement required to achieve our goal. Furthermore, a fully autonomous wireless version of the NanoWalker will prove to be essential to avoid congestion when several robots operate within the same space.

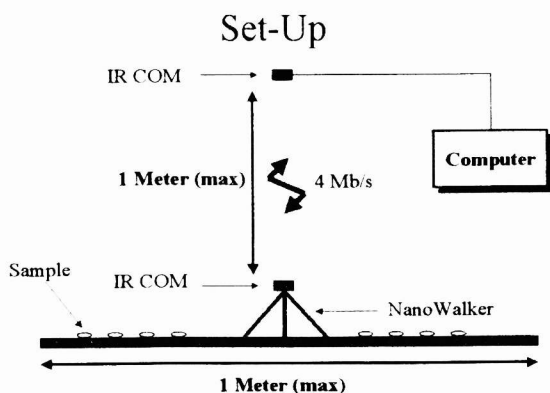


Fig. 3 - Wireless communication set-up.

As such, we have decided to implement a fast infrared (FIR) communication scheme as shown in Fig. 3. The FIR technology allows half-duplex wireless communication to be performed at 4 millions bits per second (Mbps) in a workspace of up to one meter in diameter. With regards to various critical aspects of the NanoWalker such as communication range, bandwidth, latency, complexity and power consumption, the FIR approach is the best and most suitable wireless technology to use at the present time. The general block diagram of the wireless communication interface is shown in Fig. 4.

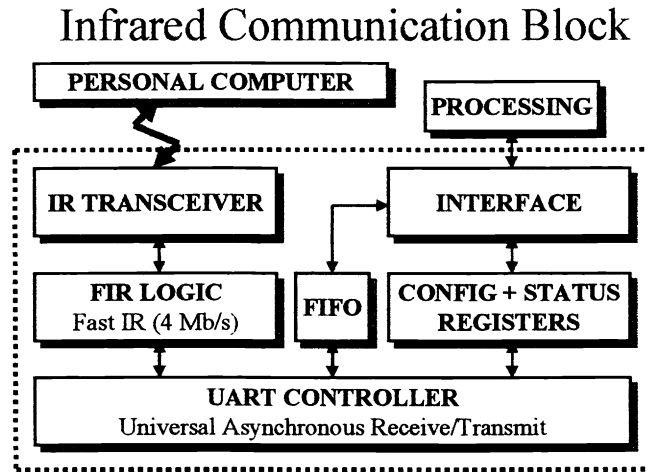


Fig. 4 - Wireless communication interface.

### 7. EMBEDDED PROCESSING

Even the simplest tasks performed by the NanoWalker require a large amount of computation to be performed within tight time constraints. For instance, a simple displacement requires the simultaneous control of the legs by generating the right voltage amplitude at the right time at the twelve electrodes connecting the electronic system to the piezo-actuators. Since in each of the 4000-10000 steps second the waveform generation process must occur and new calculations must be performed for each electrode at each step, the additional latency caused by the wireless communication and the personal computer is a serious limitation to the performance of the NanoWalker. Hence, a 50 MIPS processing block (limited to 48 MIPS in the present design) is integrated into the NanoWalker. The processing block includes a digital signal processor (DSP) with non-volatile RAM based on flash technology, and a fast volatile RAM block. The general block diagram is shown in Fig. 5.

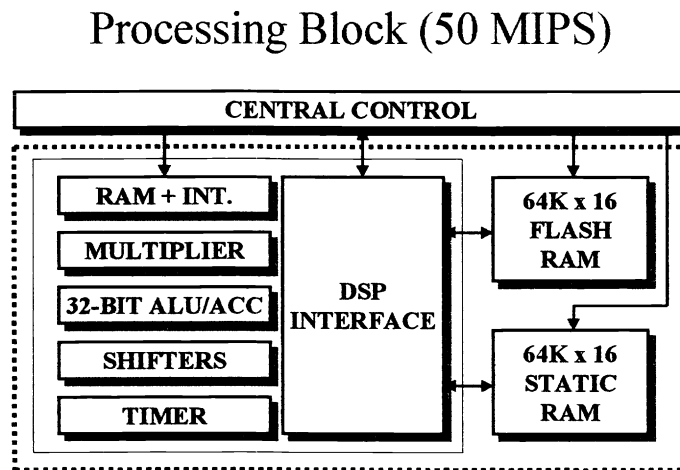


Fig. 5 - Embedded processing block.

## 8. PIEZO-ACTUATOR INTERFACES

The function of the piezo-actuator interfaces is to convert each command from the embedded processor to an analog voltage suitable for the piezo-actuators. Each NanoWalker requires four piezo-actuator interfaces, three interfaces for the legs and one interface for the instrument, initially the STM<sup>2</sup>. This is shown in Fig. 6.

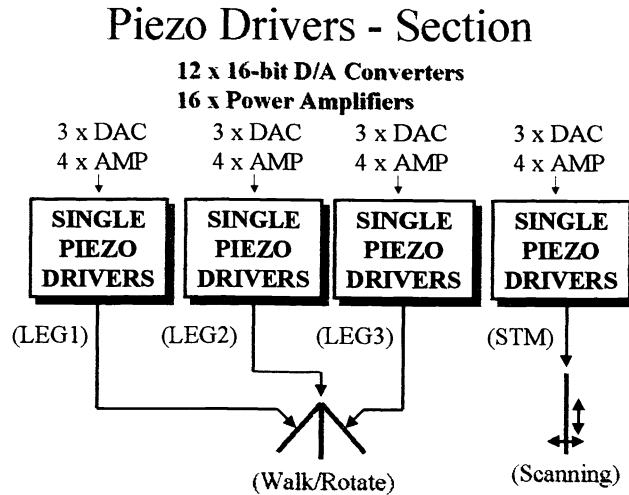


Fig. 6 - Piezo-driver interfaces for each NanoWalker.

Fig. 7 shows the basic configuration of a single piezo-driver interface. This configuration allows the number of DAC devices per leg to be decreased from four to three. For each leg, the embedded processor writes the calculated digital values for the x, y, and z coordinates to the three respective 16-bit DAC devices in one of the four piezo-driver interfaces. Because the analog signals  $V_x$ ,  $V_y$ , and  $V_z$  at the outputs of the DACs are within the  $\pm 5$  Volts which is insufficient to drive the piezo-actuators, four power amplifiers are used to boost the signals to  $\pm 88$  Volts. This voltage is the maximum possible output swing when power rail voltages of  $\pm 100$  Volts are applied to these power amplifiers. To maximize the effect on the piezo-tubes, each electrode has a counter-electrode located on the opposite side of the piezo-tube (the inner piezo-tube is grounded). The counter-electrode receives the same voltage as its respective electrode but with inverse polarity. This is automatically done in analog form through the power amplifiers. The  $V_z$  component is also included in all power amplifiers' outputs to avoid an additional DAC in the configuration.

### Single Piezo Drivers

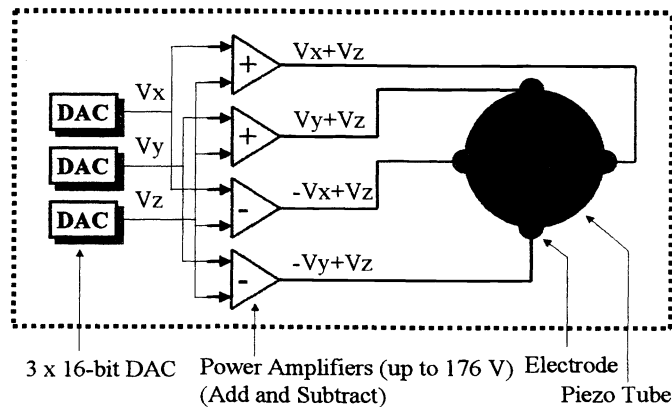


Fig. 7 - Layout of a single piezo-driver interface.

## 9. INSTRUMENT INTERFACE

The instrument interface is a key element of the NanoWalker. It allows various instruments to be interchangeable. Because of the very small size and the tight tolerances, the task is quite challenging. As shown in Fig. 8, the interface consists of a special electronic block with both an electronic and a special instrument port (described in the next section). The interchangeable instrument is connected to the NanoWalker mechanically through the instrument port and fixed in position by a special clamping configuration. A miniature cable provides all electrical links between the interchangeable instrument and the electronic block embedded in the NanoWalker.

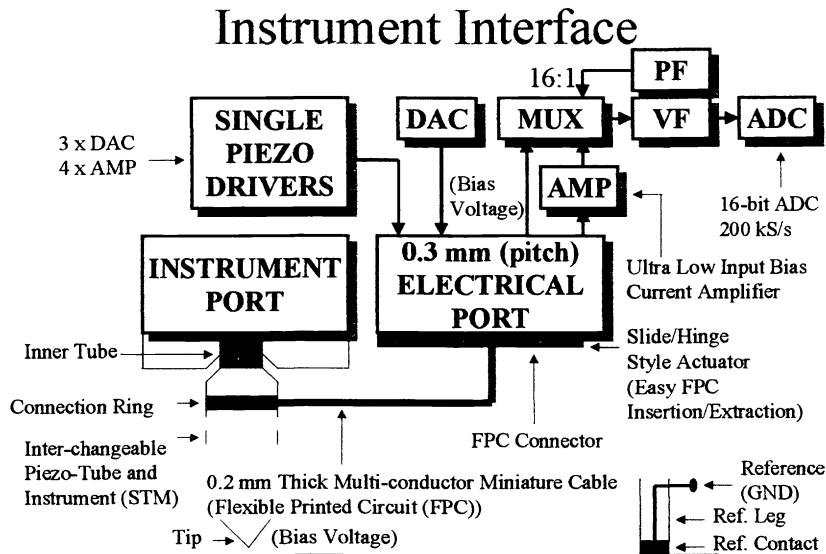


Fig. 8 - Block diagram of the instrument interface.

In Fig. 8, the electrical port provides the electrical connections to the interchangeable instrument through a FPC-based 0.2 mm thick multi-conductor miniature cable especially designed for this purpose. The cable permanently connected to the interchangeable instrument is easily inserted or extracted to/from a 0.3 mm pitch connector equipped with a miniature slide/hinge style actuator. The cable can carry the signals (for raster scan in STM applications) from the dedicated single piezo-driver interface as shown in Fig. 8 or Fig. 6 where the configuration is the same as the one depicted in Fig. 7.

The output of a 16-bit DAC provides the programmable bias voltage. The bias voltage and the grounded surface are required for generating the tunneling effect at the tip of the STM. The tunneling current is fed back through the miniature cable and the electrical port to an ultra low input bias current amplifier, which converts the tunneling currents into voltage amplitudes. The output of the low input bias amplifier is routed to one of the sixteen inputs of an analog multiplexer (MUX). Another input of the multiplexer is connected to a power feedback (PF) circuit used to alarm the on-board processor when the batteries are closed to being in the discharge state. 14 analog inputs remain accessible through the electrical port for general use. The output of the analog multiplexer is connected to a 200,000 samples per second (K.S/s) 16-bit A/D converter (ADC) through a voltage follower (VF) to provide the low-impedance driving source required at the input of the ADC.

## 10. INSTRUMENT PORT

The instrument port is shown in Fig. 9. An inner tube permanently attached to the interchangeable instrument (the piezo-ceramic tube for the STM for instance) is allowed to slide inside the instrument port piezo-ceramic tube permanently attached to the NanoWalker mechanical structure. Two circumference bands (isolation layers in Fig. 9) are machined on the initial conductive material plated on the outer and inner surfaces of the instrument port piezo-tube resulting in six circumference electrodes and three rings: the upper ring, the middle ring, and the lower ring as depicted in Fig. 9.

The relatively flat upper and lower rings are used as micro-clamps while the middle ring is used to move the inner tube up and down. A 16-bit DAC with two power amplifiers provide up to 176 Volts to each micro-clamp. Maximizing the voltage available at the micro-clamps can be critical for potential instruments having extra weight. The middle ring is used for fine z-

axis (vertical) displacement of the instrument or a potential nano-manipulator. As such, only one inverting power amplifier has been implemented following a 16-bit DAC. The inner electrode E2' is connected to ground in order to achieve a lower displacement increment within the dynamic range of the voltage applied to the piezo-tube.

Since for a given electric field, the vertical length of the piezo-tube determines the magnitude of the extension or contraction in the z-axis, the configuration depicted in Fig. 9 provides us with three levels of adjustment in the z-axis. The instrument piezo-tube provides a coarse control and the middle ring, which is shorter than the STM piezo-tube but longer than the micro-clamps, provides a much finer control. The difference between 88 Volts and the required clamping voltage can also be used for the finest adjustment in the z-axis using one of the two clamps.

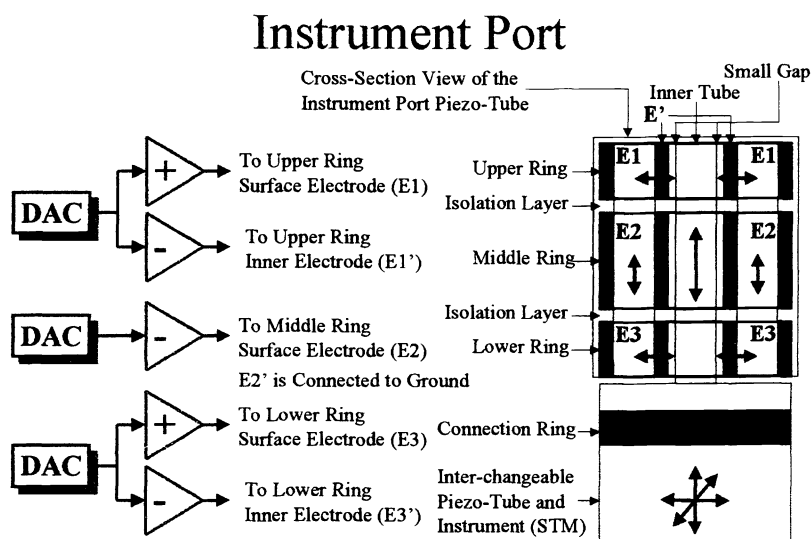


Fig. 9 - Diagram of the instrument port.

The STM piezo-tube and its attached inner tube are typically completely inserted within the instrument port piezo-tube to avoid damage of the sensitive tip of the SCM by contact with the surface. Then if not enough friction is available to maintain the instrument, a high voltage is applied to one of the micro-clamps to retain the inner tube.

The tip can be positioned by clamping the inner tube with the lower ring while unclamping with the upper ring. Then a voltage is applied to the middle ring to extend upward the instrument port piezo-tube. Then the inner tube is clamped with the upper ring and released with the lower ring. This step can be repeated as necessary. Motion of the STM tip upward is simply achieved by reversing the sequence.

Coarse positioning as well as raster scan can also be achieved through the STM piezo-tube by sending the appropriate voltage amplitudes through the connection ring as depicted in Fig. 9. The position of the tip when approaching the surface is simply determined by the tunneling current, which is fed back to the on-board processor.

## 11. CENTRAL CONTROL BLOCK

Miniaturization and performance can be achieved through a high level of integration by replacing several electronic components with a single complex programmable logic device<sup>3</sup> (CPLD) generally referred to as the NanoWalker controller or technically referred to as the NW95144XL-7. This device is powered at 3.3 V and contains the control electronics partitioned among 144 macro-cells to synchronize and interconnect components together as well as providing processor access control, decoding, interrupt support, expansion port, and the integration of a special decoding scheme to re-program the on-board flash memory.



The device uses an advanced 0.6  $\mu\text{m}$  CMOS flash process. The NW95144 uses chip-scale packaging (CSP), the smallest packaging technology after the die form, to provide 144 connection points within a 12.0 mm  $\times$  12.0 mm surface area. All functions within the device are executed simultaneously in less than 7.5 nanoseconds (worst case). The full development and design of the NW95144 has been done using the most advanced design methodology based on hardware description language<sup>4</sup> (HDL) with both behavioral and structural modeling. Translation to a gate-level implementation has been done through advanced computer-based synthesis processes. Computer-assisted optimization has been conducted and the entire design functionality and timing characteristics have been verified and validated through extensive simulation.

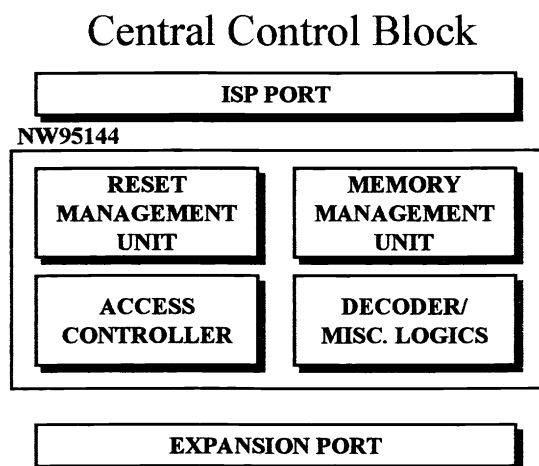


**Fig. 10** - Basic block diagram of the central control block.

For simplicity, the NanoWalker controller can be divided into four main units as depicted in Fig. 10. The reset management unit (RMU) recognizes three types of resets: a power-reset, a self-reset, and a force-reset. In the power-reset mode, the RMU maintains the system in reset mode until the power is completely stabilized. The self-reset mode allows the embedded processor to reset the entire system and to reboot itself. A force-reset is used prior to in-system programming (ISP) and testing. It can be applied from an external device through the ISP port.

The access controller is used for timing and synchronization including wait-states control for the accesses performed by the embedded processor. The memory management unit (MMU) is used mainly for memory shadowing. Shadowing refers to the copying of read-only memory (ROM)-based memory into the same addresses in main RAM. Since RAM is typically faster than ROM-based memory, successful shadowing improves system performance. The ROM-based memory of the NanoWalker is implemented with 120 nanosecond (ns) access time flash RAM while the SRAM has an access time as low as 15 ns. Although the content of the flash RAM can be updated by writing to it, the writing process is too complex and time consuming to be used during normal execution phase and only read accesses would typically be performed during such time. Both SRAM and the flash RAM occupy the same address space and shadowing can be performed on eight different memory sectors with an average size of 16 KB per sector. The MMU can also be used for sector swapping and loading additional user's codes through the IR link to one or more sectors in the flash or SRAM space.

The last main unit of the NanoWalker consists of a decoding block and a miscellaneous logic block. The decoder maps the embedded processor's accesses to the right peripheral devices. The miscellaneous logic block performs several smaller tasks including shutdown controls (Section 13) that otherwise would require additional logic components to be implemented.

Besides the NanoWalker controller unit, the central control block has an ISP port and an expansion port. The ISP port has been especially designed to accept a special proprietary emulation cable. This allows the NW95144 to be re-programmed through an embedded Joint Test Access Group (JTAG) interface by using the boundary-scan path within the device. It also allows the flash RAM to be pre-programmed. Although the embedded processor can re-program the flash RAM with codes received through the IR link, since no codes exist initially in the flash RAM, the embedded processor cannot boot. To resolve this issue, the emulation cable is connected to the ISP port, the force-reset is applied momentarily and the codes from a personal computer are written to the flash RAM through the NanoWalker internal bus using the processor emulation facility

embedded in the cable. While doing so, special control on the emulation cable forces the pins of the embedded processor connected to the internal bus to remain in a high-impedance state to avoid conflicts. For testing purpose, the emulation cable is also designed with special ports that allow a logic analysis system to capture timing waveforms and states directly from the NanoWalker internal bus while in execution mode.

The expansion port provides additional connections for future expansion where most of the available connections can take advantage of the internal programmable gates available in the NanoWalker controller. The ISP and the expansion port are each implemented with a 0.3 mm pitch 51-pin FPC-connector in surface-mounted technology (SMT) with zero insertion force (ZIF) and has an overall length of 17.7 mm, slightly less than the length of a piezo-actuator leg.

## 12. POWER SOURCE

After investigating, we selected special rechargeable 6-Volt lithium-metal cells as the power source for this version of the NanoWalker. Our primary concern with regards to integrating batteries on the NanoWalker was the significant additional weight. Fortunately, past experiments conducted in our laboratory have shown that the NanoWalker could carry an extra weight of > 200 grams (more than 100 times the weight of its own mechanical frame) and was still capable of relatively fast motion. Both walking and rotating motion at > 2 mm/s have been achieved at voltage amplitudes applied to the piezo-actuators as low as  $\pm 40$  V. With the embedded capability of applying voltage amplitudes of at least twice these values, additional weight can be applied or faster displacement can be achieved.

With all this functionality embedded in the robot, the electronics also require a fair amount of continuous current to operate. Although exact data will be computed with the prototype system, a rough estimation of continuous current required to operate the system in the worst case conditions, is shown in Table 1.

Main Sections	Estimated Maximum Current (mA)	% of NanoWalker Consumption
IR Communication Interface	600	23
Processing, Memory, and Clock	300	11.5
Central Controller	300	11.5
A/D and D/A Conversion Blocks	50	2
Power Amplifiers for the 3 Legs	770	30
Power Amplifiers for Instrumentation	580	22

Table 1 - Estimated continuous discharge current required in worst case conditions.

Table 1 indicates that about half of the approximate 13 W of power is consumed by the power amplifiers driving the piezo-tubes for the three legs, the removable instrument, and the instrument port. As mentioned previously, the piezo-actuators consume virtually no power. Most of the power is consumed by the quiescent current flowing through the power amplifiers. Specifically, the quiescent current was measured at  $\pm 5$  mA (at  $\pm 100$  V) per leg. Since the moving speed of the NanoWalker has no significant impact on the power consumption when the amplifiers are powered, the best strategy is to move and perform operations at the maximum possible rate within the operational time, i.e. until the batteries are discharged. A strategy to decrease significantly the power consumption is to power only a subset of the power amplifiers at any given time. For instance, displacements such as walking or rotating are not being done at the same time as scanning with the STM. The quiescent current to drive the three legs alone for walking or rotating contribute to about 30% of the whole power consumption while the power amplifiers attached to the instrument port and the STM contribute to about 22% of the whole power consumption. By shutting down the power through on-board N-channel power MOSFETs to one of these two power amplifiers sections, significant saving in power consumption can be achieved.

Nonetheless, despite this "shutdown" feature set through the NW95144, the battery technology must still be carefully evaluated. Although the lithium-metal cells have the largest energy density among all batteries available, the 6 V output voltage created by two 3 V cells in series barely provide the minimum required voltage to be adequately regulated for proper operation of the embedded electronic system. Although the cell's discharge characteristic is relatively flat, the battery configuration must be implemented such that the output voltage during the whole discharge period remains sufficiently high in order to eliminate any risks of system failures. Although the preliminary design of the cell has been done, other aspects such as the final physical shape and size as well as determining the dynamic characteristics, will be completed later once new data has been obtained with our prototype system.

As a first estimate, six 6 V lithium/manganese dioxide (Li/MnO<sub>2</sub>) batteries, each comprised of two 3 V cells in series, will have a total rated capacity of 8,400 mAh at 200 ohms (Ω) to 4.0 V at 20°C. This would correspond to a total battery weight of 240 grams, which is from past experiments, the total weight that should be reserved for the batteries. This would correspond to approximately 10 Ω of load or 520 mA of drain current per battery, which would translate to approximately 1 hour of continuous operation. The drawback is the volume occupied since each battery requires 21.7 cm<sup>3</sup>. A simple example is the DL245 battery<sup>5</sup> with approximate dimensions of 45mm × 34 mm × 17 mm. An example of a possible implementation is shown in Fig. 11.

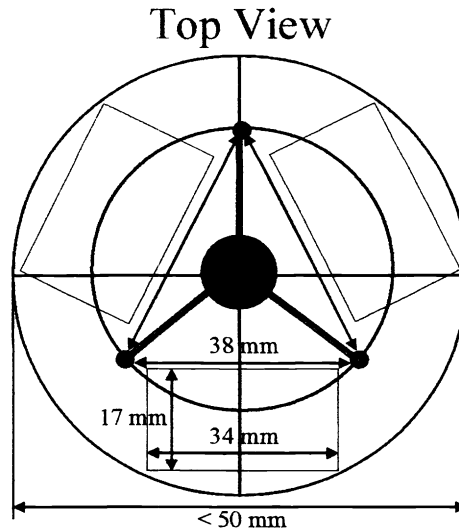


Fig. 11 - Possible approximate NanoWalker dimensions with the batteries.

Because of the weight, three batteries could be installed at the base of the NanoWalker to maintain a good stability of the whole structure at the expense of increasing the surface area occupied by the NanoWalker, but which could be maintained below 50 mm in diameter. The total height of the NanoWalker with three batteries for approximately 30 minutes of continuous operation would be approximately 50 mm being approximately 32 mm above the top of the actual mechanical frame. Adding three more batteries on top of the three batteries shown in Fig. 11 to achieve 1 hour of continuous operation would bring the total height to approximately 100 mm. This would still offer adequate structural stability in good environmental conditions.

### 13. POWER DISTRIBUTION BLOCK

The power distribution block is shown in Fig. 12. The unregulated output from the Lithium cells is connected through a micro mechanical switch (SW) to a voltage regulator (REG) to provide the NanoWalker main power rail of +5 VDC. This voltage is used to power various parts of the NanoWalker including the IR interface and the computation block.

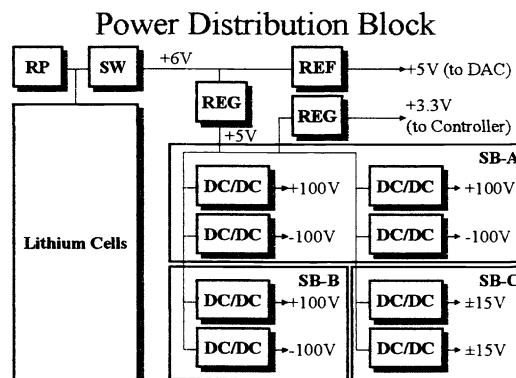


Fig. 12 - Power distribution block.

Because of switching noises on the main power rail, another +5 VDC is also generated through a voltage reference circuit. This low noise +5 VDC is used by all DACs for conversions (the ADC has an internal reference). The micro mechanical switch is used to power down the NanoWalker as necessary. Two recharge pads (RP) are also available to recharge the cells while resident in the system. The main power rail is further regulated down to 3.3 VDC to supply the NanoWalker controller. The main power rail voltage is also increased through eight DC-to-DC (DC/DC) partitioned among three sub-blocks: SB-A, SB-B, and SB-C as depicted in Fig. 12. Each DC/DC converter occupies a volume of 12.72 mm × 12.72 mm × 8.64 mm.

The SB-A sub-block is used to provide the power rails for the amplifiers driving the three legs. Four single-output DC/DC converters are used, each capable of supplying a maximum of 12.5 mA. Four voltage converters instead of a single converter were more attractive in our case to ease integrating all components within the smallest possible volume. The SB-B sub-block provides the power rails for the amplifiers driving the instrument (STM and instrument port piezo-tube) while the ± 15V dual-output DC/DC converters in sub-block SB-C are used to power all the DACs.

#### 14. MICRO-ELECTRONIC ASSEMBLY

With more than 600 electronic components, traditional assembly techniques even based on the most recent and smallest packaging techniques such as CSP would result in a final implementation too large to fit in the NanoWalker. In order to achieve the smallest implementation, packaging has been simply eliminated for most parts by connecting the electronic dies directly to a Kapton-based FPC. Modern hybrid systems such as multi-chip modules<sup>6</sup> (MCM) typically achieve small size by connecting dies to a substrate with wire bonding techniques. Wire bonding uses critical space surrounding the die for connections. We are using a more recent assembly technique called flip-chip technology where the die is bumped by soldering tiny gold balls. Once the bumping process has been done, the die is simply "flipped", aligned, and fixed to the substrate, eliminating the connection area surrounding the die.

#### 15. CONCLUSION

The main components of a small wireless robot capable of carrying various instruments or nano-manipulators have been presented. The robot based on piezo-actuators and is capable of sub-atomic movements. It was also shown that a fairly complex electronic section must be embedded in the robot using the most advanced packaging techniques. Despite the complexity of such a system, we demonstrated that it is possible to implement the NanoWalker robot within very small dimensions. The resulting NanoWalker robot should provide a highly integrated autonomous platform to install micro-devices for a new generation of measurement and inspection systems.

#### 16. ACKNOWLEDGEMENTS

This project is presently supported by the Seaver Institute. The authors also wish to acknowledge the support of Analog Devices, Inc. in providing several key components. The STM laboratory at the Institute of Physics and Astronomy, University of Aarhus in Denmark provided us with valuable information used in the design of the instrument port.

#### 17. REFERENCES

1. L. Sosnowski, "Piezo actuated nano-stepping micro-robot chassis design and control", Undergraduate thesis, Bio-instrumentation Laboratory, Massachusetts Institute of Technology, 65 pages, 1998.
2. C. Chen, "Introduction to scanning tunneling microscopy", New York: Oxford University Press, 1993.
3. "XC95144 in-system programmable CPLD", Data Sheet, Xilinx, Inc., 1998.
4. K. Skahill, J. Legenhausen, R. Wade, C. Wilner, and B. Wilson, "VHDL for programmable logic", Addison-Wesley Pub. Co., 593 pages, 1996.
5. "DL245 Lithium/Manganese Dioxide Battery", Data Sheet, Duracell, Inc., 1993.
6. G. Ginsberg and D. Schnorr, "Multichip modules and related technologies: McM, Tab, and Cob design (electronic packaging and interconnection series)", McGraw Hill, 1994.

---

For further information, comments, and/or interest in collaborative researches in any areas pertinent to this project - Correspondence: Sylvain Martel, Ph.D., Postdoctoral Research Associate, Bio-Instrumentation Laboratory, Massachusetts Institute of Technology, 77 Massachusetts Ave., Room 3-147, Cambridge, MA, USA, 02139.  
Email: [smmartel@mit.edu](mailto:smmartel@mit.edu)